Collapse structures on seismic in Flanders

Introduction

The Campine Basin in eastern Flanders is defined by the presence of Upper Palaeozoic deposits on top of a strongly deformed lower Palaeozoic basement. The Upper Palaeozoic deposits are unconformably overlain by several hundred meters thick Upper Cretaceous and Cenozoic strata.

A dense network of 2D seismic lines of different age and strongly varying quality are present in the Campine basin. On specific sets of seismic data in the western Campine Basin, Dreesen et al. (1987) and De Batist & Versteeg (1999) observed the local occurrence of major depressions in Carboniferous, Upper Cretaceous and Paleogene strata. The authors presumed that the depressions represent collapse structures in the Dinantian limestones.

In order to construct the new 3D geological model of Flanders (G3Dv3-model; Deckers et al., 2019), the seismic dataset used by Dreesen et al. (1987) and De Batist & Versteeg (1999) was extended to include all available seismic lines in the Campine Basin. On these seismic lines several horizons, among which the top of the Dinantian and overlying bases of the Westphalian, Upper Cretaceous, Paleogene were interpreted. The extension of the seismic dataset and interpretations hence allowed a new, more comprehensive study of the collapse structures. In this factsheet, we discuss our findings on the locality, geometry, timing and mechanism behind the collapse structures.

Locality and geometry

A total of 45 collapse structures have been mapped on seismic data. This is an underestimation as only the biggest collapse structures have been interpreted, and in many areas there is only limited seismic data coverage. Indeed, on gravimetric maps several more collapse structures, which coincide with negative bouguer anomalies, could be observed (Debacker et al., 2018). The collapse structures are expressed by local depressions in the Namurian, Westphalian and to a lesser extent the Upper Cretaceous and Paleogene strata. They can be recognized on the seismic data as, often symmetric, sag structures with related sharply downwards dipping reflections towards their centre (Figure 2). The structures penetrate the top of the Dinantian limestones and seem to diminish within these limestones .

Figure 1 shows that most of the collapse structures are clustered in the (south)western part or border area of the Campine Basin. Here, the Dinantian is overlain by several hundred meters of Namurian and Westphalian strata below the Upper Cretaceous/Cenozoic coverage. Further towards the northeast, the Namurian and Westphalian strata thicken and the number of collapse structures rapidly decreases. At the southern border of the Campine Basin no major, and also less collapse structures were observed (Figure 1). The size of the collapse structures strongly varies. The estimated lateral and vertical extent of these structures are shown in Figure 1. Maximum vertical extents are thought to reach over 200 meters, and maximum horizontal extents of the circular to ellipsoid structures are 1500 by 5000 meters. The throw of the collapse structures has been measured at four levels, namely the top Dinantian, base Westphalian, base Cretaceous and base Cenozoic, and are shown in the data table included at the end of this factsheet. Main uncertainty on the lateral and vertical extent is related to the often limited amount of seismic lines crossing these structures.

The collapse structures are generally located near or on top of faults. These are all normal faults that were formed during the Jurassic extensional phase, some of which were (re)activated during the Cenozoic. Some collapse structures are located within narrow graben structures. In these cases, it is often difficult to distinguish the displacement that

This file is part of the GeoConnect³d project that has received funding by the European Union's Horizon 2020 research and innovation programme under grant agreement n.731166.

is related to the throw along the faults that bound the graben, and the displacement that is related to the collapse. The dominant Meso- and Cenozoic fault strike in the area is NNW-SSE and WNW-ESE according to the G3Dv3-model (Deckers et al., 2019). The collapse structures are therefore often aligned along these directions (Figure 1). Interesting is a potential (W)SW-(E)NE alignment of a number of collapse structures (Figure 1), as it is almost perpendicular to the Meso- and Cenozoic fault directions.

The relationship of the collapse structures to one or more faults from the Structural Framework is added in the table at the end of the factsheet, as well as their visibility on the bouguer gravity anomaly map (Debacker et al., 2018) and whether their seismic interpretation is certain or not.

Mechanism

Dreesen et al. (1987) related the collapse structures in the Dinantian to dissolution of evaporites within the Dinantian. In the wells in the Dinantian of the Campine Basin, however, no evaporite layers were encountered. The evaporites could therefore have been missed, or have already been dissolved at the borehole locations. Several breccia levels were encountered which could possibly support the latter hypothesis, but further research is needed to elaborate whether they are indeed related to evaporite dissolution. At the southern flank of the Brabant Massif, in the Mons area, collapse structures were observed in the Dinantian that were clearly relatable to dissolution of evaporites (Rouchy et al., 1987). Given their proximity and similar paleogeographical setting, it is likely that evaporites were also deposited along the northern flank of the Brabant Massif or in the Campine Basin and that the collapse structures there can also be related to evaporite dissolution. Furthermore, the main collapse structures in the Campine Basin occur in a restricted area which is bordered by the Brabant Massif in the south and west and based on seismic data by a Dinantian reefal belt towards the north and east, generating the ideal circumstances for a periodically isolated and evaporating inland sea during sea level low stands, or a similar mechanism as described for the Mons Basin by De Putter et al. (1994). In the Saint-Ghislain borehole in the latter area, Dinantian evaporite succession of 350 meters thickness were encountered. Similar Dinantian evaporite thicknesses are necessary in the Campine Basin to cause the observed vertical extent of some of the observed collapse structures of over 200 meter. Dissolution of the evaporites was probably enabled by extensive fluid flow along major faults. This explains the close association of collapse structures and the major faults in the Campine Basin.

This file is part of the GeoConnect³d project that has received funding by the European Union's Horizon 2020 research and innovation programme under grant agreement n.731166.

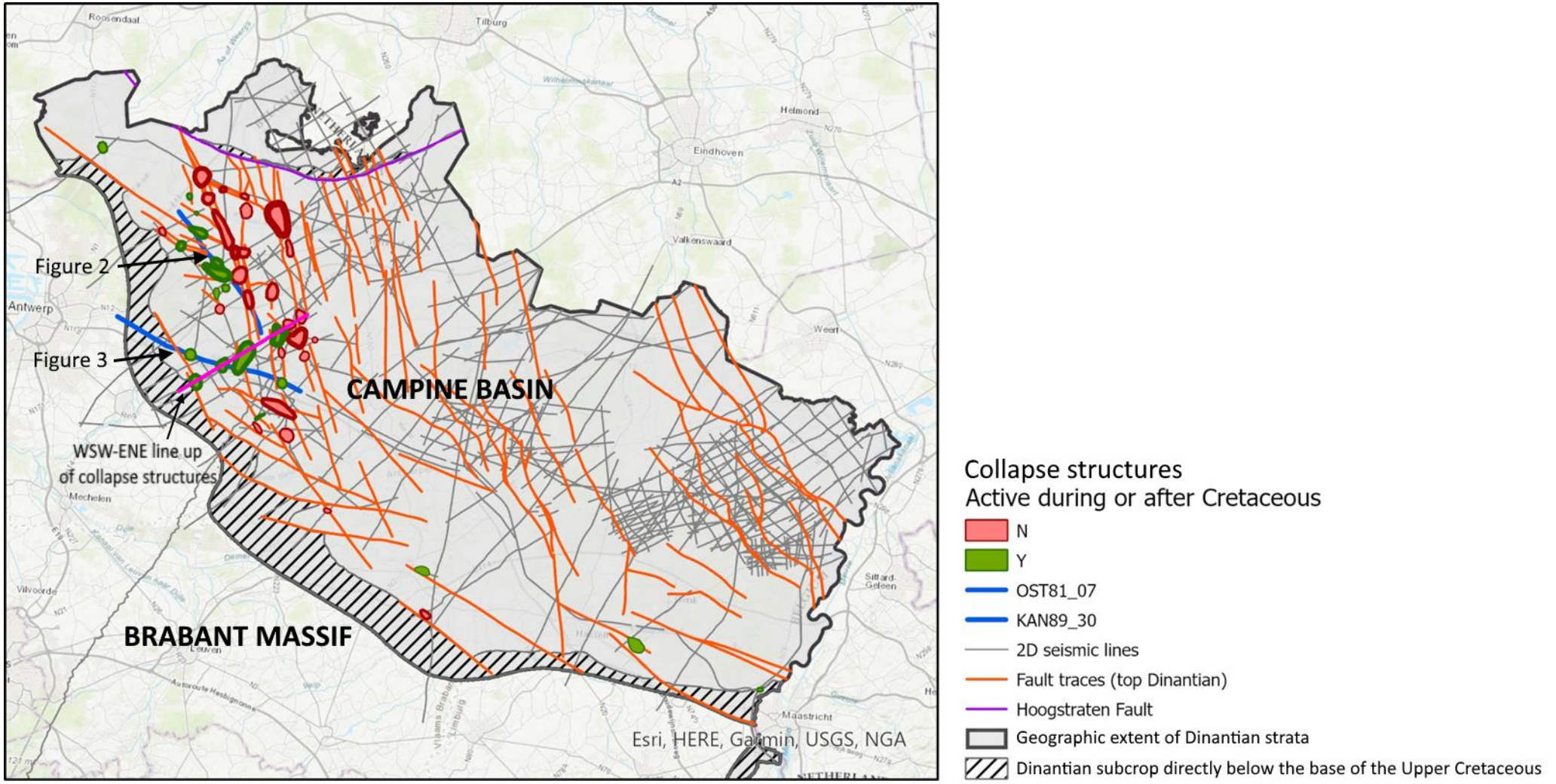

Figure 1 : Overview of the mapped collapse structures in red and green based on 2D seismic data (shown as grey lines). Green polygons mark collapse structures that reach into the Paleogene. Red polygons reflect collapse structures in the Carboniferous that are vertically delimited by the base Cretaceous unconformity The vertical throw of the collapse structures is indicated by the thickness of the contour lines: the thicker the line the larger the throw. Orange lines are major faults that were mapped for the G3Dv3-model at the top Dinantian level and are included in the Structural Framework of GeoConncect³d. The seismic lines shown in figure 2 (upper NW-SE line) and 3 (lower WNW-ESE line) are indicated in blue.

This file is part of the GeoConnect³d project that has received funding by the European Union's Horizon 2020 research and innovation programme under grant agreement n.731166.

Timing

The collapse structures have different upper limits: some die out just above the top of the Dinantian, whereas others continue into the Paleogene (Figure 2 and 3). The upper limits of the collapse structures are not random, but bounded by some of the major unconformities which coincide with the main tectonic phases. We identified three main surfaces by which the collapse structures are topped:

- Several small collapse structures are limited to the lowermost part of the Namurian, just above the top of the Dinantian. These structures can be related to dissolution in the top of the Dinantian when it was aerially exposed just after deposition (Vandenberghe en Bouckaert, 1980). During the subsequent Namurian transgression, these collapse structures were filled. Such small collapse structures, that only developed during an upper Dinantian to lower Namurian hiatus, have not been mapped, as they are limited in vertical and lateral extent. Most of them are probably below the resolution of the seismic data.
- Most collapse structures are topped by the base of the Upper Cretaceous which unconformably overlies the Upper Carboniferous strata (collapse structure on the right in Figure 2). This means that collapse occurred sometime during the large hiatus between the Upper Carboniferous and Upper Cretaceous. As this is such a large hiatus, it is difficult to establish an exact timing for the dissolution phase(s). However, in the Mons area, a major dissolution phase also occurred during this hiatus, which was dated late Early Cretaceous by Quinif et al. (2006). Swennen et al. (2021) also showed that a vein in the Heibaart borehole in the western Campine Basin yielded an age of 113.0 ± 2.6 Ma. This makes a late Early Cretaceous age for a major dissolution phase in the Campine Basin very likely.
- A number of collapse structures continue into the Upper Cretaceous and Paleogene. The majority of the collapse structures that continue through the Upper Cretaceous, also continue through the Paleocene-Eocene boundary and are topped by the base Oligocene reflector (Figure 3). A similar observation was made by Debatist & Versteeg (1999). Since the region experienced large wavelength deformation by the Pyrenean tectonic phase just before the onset of the Oligocene (Deckers et al., 2016), it is likely that dissolution and renewed collapse was related to this phase. The earlier, middle Paleocene Laramide tectonic phase shares similar dynamics as the Pyrenean tectonic phase (Deckers & van der Voet, 2018) and could therefore also have contributed to this Paleogene collapse episode, especially since fracture-filled veins of this age were detected in a drilled section of the Dinantian in the region by Swennen et al. (2021).

This file is part of the GeoConnect³d project that has received funding by the European Union's Horizon 2020 research and innovation programme under grant agreement n.731166.

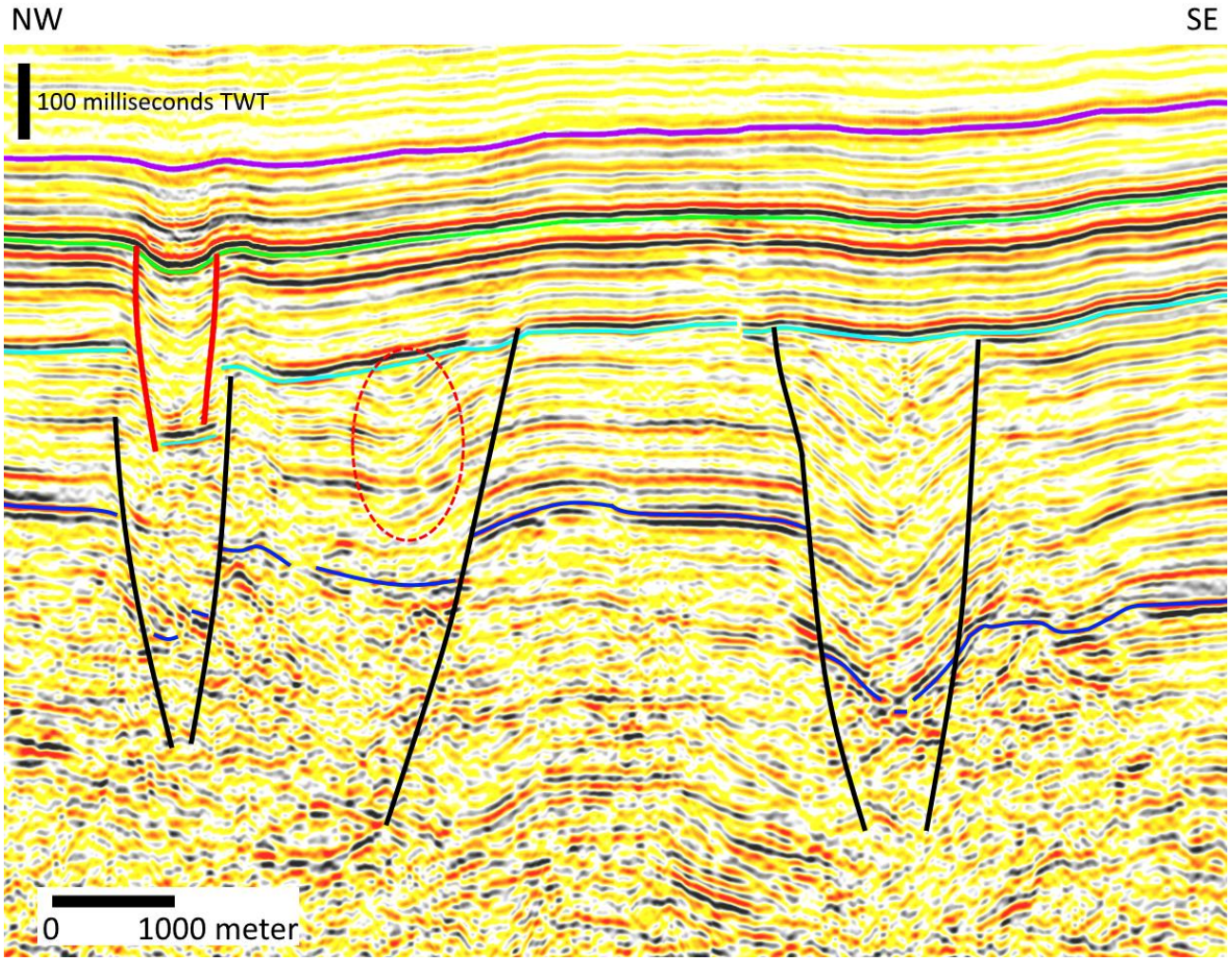

Figure 2: Seismic line 8107 (location see Figure 1) from the reprocessed 1981 Oostmalle campaign showing two major graben related collapse structures. In between these major collapse structures a third collapse structure can be observed (indicated by a red circle) which seems to not reach the top Dinantian. This third structure represents the flank of a major collapse structure further west that does penetrate the Dinantian. Base Upper Cretaceous and top Dinantian are indicated in light and dark blue, base Paleogene in green, Paleocene-Eocene boundary in purple, faults in top Dinantian in black, and faults related to collapse in red. Notice that the collapse structure on the left continues through the Upper Cretaceous into the Paleogene, whereas the one on the right ends at the base of the Upper Cretaceous. .

This file is part of the GeoConnect³d project that has received funding by the European Union's Horizon 2020 research and innovation programme under grant agreement n.731166.

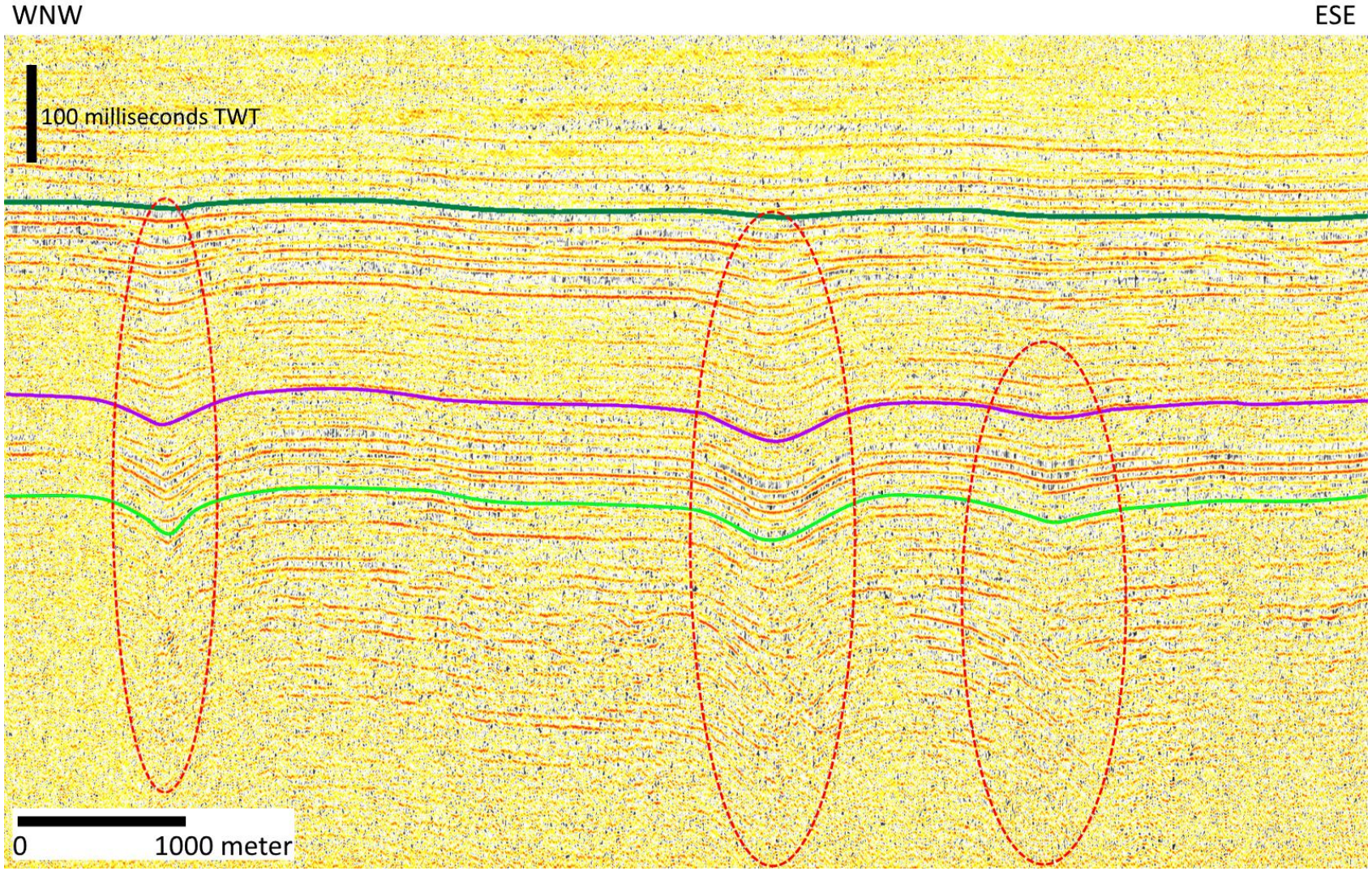

Figure 3: Seismic section 30 (location see Figure 1) from the Channel seismic 1989-1996 campaign showing three collapse structures affecting Paleogene layers. Base Oligocene, base Eocene and base Paleogene are indicated by dark green, purple and light green lines, respectively. Base Upper Cretaceous and top Dinantian could not be interpreted on this line as it only sufficiently images the Cenozoic layers.

This file is part of the GeoConnect³d project that has received funding by the European Union's Horizon 2020 research and innovation programme under grant agreement n.731166.

Data

Number	Top Dinantian (Mean throw)	Base Westphalian (Mean throw)	Base Upper Cretaceous (Mean throw)	Base Paleogene (Mean throw)	Fault related? *Yes = fault related, but not mapped; fault number(s) of the Structural Framework*	Visible on gravimetry	Active during Upper Cretaceous/ Paleocene	Interpretation on seismic uncertain
	Milliseconds TWT	*Milliseconds TWT*	*Milliseconds TWT*	*Milliseconds TWT*				
1	90	90	82.5	57.5	Breuk_129	Yes	Yes	
2	45	NP	limited	0	Breuk_38, Breuk_97	No	No	
3	NI	NI	47.5	30	Breuk_5	No	Yes	
4	NI	85	40	35	Yes	Yes	Yes	
5	37.5	27.5	22.5	12.5	Yes	No	Yes	
6	117.5	72.5	20	15	Breuk_98	Yes	Yes	
7	120	87.5	47.5	22.5	Breuk_72, Breuk_74, Breuk_93	Yes	Yes	
8	22.5	20	15	10	Breuk_23	No	Yes	
9	45	30	0	0	Yes	No	No	
10	30	0	0	0	Yes	No	No	
11	70	57.5	0	0	Breuk_46	No	No	
12	47.5	25	0	0	Yes	No	No	
13	92.5	77.5	0	0	Breuk_90	Yes	No	
14	37.5	30	0	0	Breuk_16	Yes	No	
15	120	97.5	0	0	Breuk_16	Yes	No	
16	40	22.5	limited	0	Breuk_23	No	No	
17	80	77.5	0	0	Breuk_28, Breuk_29	No	No	
18	NI	50	0	0	Breuk_16; Breuk_28	No	No	
19	37.5	25	0	0	Breuk_25	No	No	
20	90	47.5	27.5	0	Breuk_38, Breuk_97	No	Yes	
21	105	105	102.5	32.5	Breuk_93	Yes	Yes	
22	125	112.5	0	0	Breuk_20, Breuk_90	No	No	
23	90	55	0	0	Breuk_20, Breuk_90	Yes	No	

This file is part of the GeoConnect³d project that has received funding by the European Union's Horizon 2020 research and innovation programme under grant agreement n.731166.

Number	Top Dinantian (Mean throw)	Base Westphalian (Mean throw)	Base Upper Cretaceous (Mean throw)	Base Paleogene (Mean throw)	Fault related? *Yes = fault related, but not mapped; fault number(s) of the Structural Framework*	Visible on gravimetry	Active during Upper Cretaceous/ Paleocene	Interpretation on seismic uncertain
	Milliseconds TWT	*Milliseconds TWT*	*Milliseconds TWT*	*Milliseconds TWT*				
24	NI	45	0	0	Breuk_119	Yes	No	x
25	NI	45	15	0	Breuk_9	Yes	Yes	
26	55	35	10	0	Breuk_18	No	No	
27	90	65	10	0	Breuk_105, Breuk 116	Yes	No	
28	85	60	0	0	Breuk_51, Breuk 52	No	No	
29	60	50	0	0	Breuk_51, Breuk 52	No	No	
30	175	160	0	0	Breuk_16, Breuk_18	No	No	
31	NI	45	15	12.5	Breuk_25, Breuk_91	Yes	Yes	x
32	NI	NP	20	15	Breuk_53	Yes	Yes	x
33	115	87.5	0	0	Breuk_20, Breuk_49, Breuk_90	No	No	
34	35	NP	0	0	Breuk_119	No	No	x
35	37.5	27.5	0	0	Breuk_11	Yes	No	x
36	75	62.5	0	0	Breuk_20, Breuk_90	Yes	No	
37	87.5	77.5	0	0	Breuk_20, Breuk_49, Breuk_90	No	No	
38	NI	NP	15	0	Breuk_120	Yes	Yes	x
39	140	57.5	15	0	Breuk_25	No	Yes	
40	52.5	45	15	0	Breuk_48	No	Yes	x
41	95	67.5	35	0	Breuk_34, Breuk_96	No	Yes	
42	60	NP	0	0	Breuk_117	Yes	No	x
43	32.5	NP	15	0	Yes	No	Yes	x
44	32.5	32.5	32.5	0	Breuk_106	No	Yes	
45	40	22.5	15	12.5	Yes	No	Yes	x

Table 1: List of the mapped collapse structures including the vertical throw at different stratigraphic levels (NI = not able to interpret at this level; NP = stratigraphic level not present). The relation to one or more faults with fault numbers from the Structural Framework, whether the collapse structure could be interpreted on the Bouguer gravity anomaly map, whether the structure was reactivated during and after the Cretaceous, and whether the interpretation on seismic is uncertain or not.

This file is part of the GeoConnect³d project that has received funding by the European Union's Horizon 2020 research and innovation programme under grant agreement n.731166.

References

De Batist M. & Versteeg W.H. (1999) Seismic stratigraphy of the Mesozoic and Cenozoic in northern Belgium: main results of a high-resolution reflection seismic survey along rivers and canals. Geologie en Mijnbouw, 77: 17-37.

Debacker, T., Deckers, J., Rombaut, B., Broothaers, M., Ferket, H. & Williamson, P., 2018. Subsurface mapping using gravity data during construction of the new 3D model of the Flemish subsurface. Abstract from 6th International Geologica Belgica meeting, 2018. Theme 3: New developments in geology and their role in future research, 7-8. https://ees.kuleuven.be/gb2018/abstracts/

Deckers J., De Koninck R., Bos S., Broothaers M., Dirix K., Hambsch L., Lagrou D., Lanckacker T., Matthijs J., Rombaut B., Van Baelen K. & Van Haren T., 2019. Geologisch (G3D) en hydrogeologisch (H3D) 3D-lagenmodel van Vlaanderen – versie 3. Studie uitgevoerd in opdracht van het Vlaams Planbureau voor Omgeving, departement Omgeving en de Vlaamse Milieumaatschappij. VITO-rapport 2018/RMA/R/1569.

Deckers, J., Vandenberghe, N., Lanckacker, T. & De Koninck, R., 2016. The Pyrenean inversion phase in northern Belgium: a relaxation inversion phase? International Journal of Earth Sciences, 105, 583-593.

Deckers, J. & van der Voet, E., 2018. A review on the structural styles of deformation during Late Cretaceous and Paleocene tectonic phases in the southern North Sea area. J. Geodyn. 115: 1-9. https://hdl.handle.net/10.1016/j.jog.2018.01.005

De Putter, T., Rouchy, J.-M., Herbosch, A., Keppens, E., Pierre, C. & Groessens, E., 1994. Sedimentology and palaeo-environment of the Upper Visean anhydrite of the Franco-Belgian Carboniferous Basin (Saint-Ghislain borehole, southern Belgium). Sedimentary Geology, 90/1-2, 77–93. https://doi.org/10.1016/0037-0738(94)90018-3

Dreesen, R., Bouckaert, J., Dusar,M., Soille, J. & Vandenberghe, N., 1987. Subsurface structural analysis of the Late-Dinantian carbonate shelf at the northern flank of the Brabant Massif (Campine Basin, N.-Belgium). Toelicht. Verhand. Geologische en Mijnkaarten van België 21, 37 pp.

Quinif, Y., Meon, H. & Yans, J., 2006. Nature and dating of karstic filling in the Hainaut Province (Belgium). Karstic, geodynamic and paleogeographic implications. Geodinamica Acta, 19/2, 73-85.

Rouchy, J.M., Laumondais, A. & Groessens, E., 1987. The Lower Carboniferous (Visean) evaporates in northern France and Belgium: depositional,diagenetic and deformational guides to reconstruct a disrupted evaporitic basin. In: Peryt, T.M. (ed.) Evaporite Basins. Lectures notes in Earth Sciences, 13: 31-67.

Swennen, R., van der Voet, E., Wei, W. & Muchez, P., 2021. Lower carboniferous fractured carbonates of the Campine Basin (NE-Belgium) as potential geothermal reservoir: Age and origin of open carbonate veins. Geothermics 96, 15 pp.

Vandenberghe, N. & Bouckaert, J., 1980. Geologische beschouwingen van geothermische mogelijkheden in Noord-Belgie. Belg. Geol. Dienst Prof. Paper 1980, 168:1-21.

This file is part of the GeoConnect³d project that has received funding by the European Union's Horizon 2020 research and innovation programme under grant agreement n.731166.

Cite this source

Rombaut, B., Deckers, J. & Dirix, K., 2021. Collapse structures on seismic in Flanders [Fact sheet]. Flemish Institute for Technological Research (VITO).

This file is part of the GeoConnect³d project that has received funding by the European Union's Horizon 2020 research and innovation programme under grant agreement n.731166.